Numerical investigation of wave-induced mean flows in the surf zone using the SPH method

Rozita Jalali Farahani
Civil Engineering Department
Johns Hopkins University
Baltimore, USA
rozita@jhu.edu

Robert A. Dalrymple
Civil Engineering Department
Johns Hopkins University
Baltimore, USA
rad@jhu.edu

Alexis Hérault
Conservatoire National des Arts et Métier
Paris, France
alexis.herault@cnam.fr

Giuseppe Bilotta
Università degli studi di Catania
Catania, Italy
bilotta@dmi.unict.it

***Abstract*— Smoothed Particle Hydrodynamics is used to model temporal and spatial variations of wave-induced nearshore circulation. An idealized rip current system consisting of a single bar and a rip channel is analysed and the interaction of rip current and waves is investigated. Numerical results include time-averaged and depth-averaged velocities as well as three-dimensional structure of flow in rip channel, over the bar and in nearshore region. Satisfactory agreement is achieved between the numerical data and laboratory measurements of Drønen et al. (2002) including mean water surface and cross-shore and long-shore velocity components.**

I. INTRODUTION

In surf zones, rip currents, often flowing seaward in gaps between sand bars, are important phenomena because of their environmental and life hazards concerns. The driving mechanism for rip currents is the momentum flux of the waves. As the waves break more on the bars and less in the rip channel, a set-up (of the mean water level) gradient occurs that drives a current towards the sea.

Haller et al. (2002) set up a series of experiments in a 17 m by 18 m wave basin. Rip current and nearshore circulation were measured over two bars and a rip channel between them [1]. Their measurements were mostly in two-dimensions, illustrating depth-integrated velocities and mean water surface elevations. The experimental results were later modelled numerically by Chen et al. (1999) [2]. They used a model based on Boussinesq equations to study nearshore circulations and compared their results with the Haller experiments. Drønen et al. (2002) performed a laboratory study of flow over a single bar and a rip channel in a 4 m wide and 30 m long wave tank. Their experiments were mostly in three-dimensional space, measuring the 3D structure of rip channel flow. Particle trajectories tests were also performed to track the particles in a rip current system [3].

This paper presents a three-dimensional numerical modelling of rip current and the associated circulations in a bar/rip channel system. The GPUSPH model [4] is extended to be capable of finding fluid parameters in fixed positions as well as from moving particles. Depth and wave-period averaging is used to determine wave-induced flows. The 3D flow pattern is studied to show the depth variation of rip current intensity. Changes of mean velocity circulations and mean water surface elevations are presented. At the end the effect of particle spacing and numerical resolution On the accuracy of results is investigated. Numerical results are compared to the experiments performed by Drønen et al. (2000).

II. GPUSPH MODEL

Implementation of the SPH method with fine resolution (large number of particles) can lead to large computational time. However, some complicated cases need a large number of particles to capture flow fields accurately. This issue leads to the use of parallel computing that has mostly been done on multiple central processing units (CPUs) of computers. Recently graphical processing units (GPUs) have been recognized as capable of parallel computing with high computational power and low expenses. GPU, because of its multi-core processors, are strongly parallel in nature and the data-parallel nature of SPH method makes it perform well on multithreaded GPU. GPU programming can be traced back to General-Purpose computation on GPU (GPGPU). This method can also use graphic programming languages such as OpenGL to provide the real-time graphic output.

Recently a new GPU parallel architecture is introduced as Compute Unified Device Architecture (CUDA), which uses high-level languages such as C, C++ and Fortran to introduce the problem to graphic cards so transfer of the problem data to GPU has become easier.

In this study, the GPUSPH package developed by Hérault et al. (2010) is implemented. It is an open-source code available from www.ce.jhu/dalrymple/GPUSPH. This package is written using CUDA programming language and is consists of two types of objects: those that are run on the CPU and the ones that are run on GPU. Data transfer from CPU to GPU and vice versa, is done in different stages of program but the main calculations are done on GPU. In

GPUSPH, the governing equations are the Navier-Stokes equation that is written as follows:

$$\frac{1}{\rho}\frac{D\rho}{Dt} + \nabla.\vec{u} = 0 \quad (1)$$

$$\frac{D\vec{u}}{Dt} = \frac{1}{\rho}\nabla P + \frac{1}{\rho}\nabla.\vec{T} + \vec{g} \quad (2)$$

where ρ = fluid particle density; $\vec{u}$ = particle density; P = fluid particle pressure; $\vec{T}$ = viscous stress tensor and $\vec{g}$ = gravity vector.

This weakly compressible SPH formulation is rendered in particle form for use in GPUSPH and an equation of state is used to predict particle pressure in each time step [5].

Different methods for modelling the fixed or moving boundary particles are applied in GPUSPH model. In the current study, the Monaghan and Kajtar (2009) boundary condition is used. They introduced a new form of radial boundary forces, which prevents fluid particles to penetrate into boundary particles. The boundary particles should have a smaller particle spacing of ratio 1/3 in comparison to fluid particles. The force per mass of fluid particle i due to boundary particle b can be written as:

$$\vec{f}_{ib} = \frac{k}{\beta}\frac{\vec{r}_{ib}}{r_{ib}^2}W_{ib}\frac{2m_b}{m_i + m_b} \quad (3)$$

where $k = gD$ and D = fluid depth ; β = a coefficient that is used so the variation of boundary particles spacing doesn't effect the fluid particle force [6].

In order to model the viscous term of Navier-stokes equation, different approaches can be used in the model. In our study, a combined SPH-LES method called sub-particle scale (SPS) is used. Large-Eddy (LES) simulation has a good reputation on modelling coherent structures in turbulent flows. A LES filtering is applied to Navier-Stokes equations to eliminate small-scale solutions. Closure sub-models are then applied to model sub-grid-scale (SGS) turbulence. The standard Smagorinsky model (1963) is used as the sub-model and the Smagorinsky coefficient is assumed to be constant. SPS method is similar to SGS scheme in Eulerian numerical methods and it improves the results in SPH method [7].

In GPUSPH model, initial data and the case configuration are first introduced to CPU and then the essential data are transferred to GPU where the main calculations take place. SPH calculations including:

- Search for neighbouring particles
- Calculation of forces using governing equations
- Calculation of pressure, velocity and position of particles in the next time step

are performed on graphic card. Then the result is transferred to CPU to be recorded as output files. OpenGL toolkit (GLUT) is also used to display real-time results so the variation of fluid parameters such as velocity, pressure and density during the computational time can be observed. GPUSPH is reported to have a one to two orders of magnitude faster computational time than the equivalent CPU code and it can be run on a single Nvidia GPU card [4].

III. FLUID PARAMETERS ON FIXED POSITIONS

While SPH as a Lagrangian numerical method has a great capability to model free surface flows with complex deformations, it is sometimes difficult to compare the results, which are available on moving particles, with experimental results which are usually measured on fixed positions. In this study, GPUSPH model is extended to find fluid parameters such as velocity, pressure and density on a set of pre-defined fixed positions. Two approaches can be considered: the first one includes more changes to the existing GPUSPH model but is more computationally optimized and can be applied for large number of fixed nodes. The second approach includes less changes to the existing code and is easier to apply but allocates excessive memory so is applicable for small number of fixed nodes.

In the first approach, the position of fixed nodes is introduced to the model through CPU and transferred to GPU using the "ParticleSystem" class of GPUSPH model. Then nodes are associated to neighbouring list cells according to their position coordinates and a hash value for each node is calculated based on its cell id using "calcHash" kernel. In the existing GPUSPH model, particles are sorted and re-ordered in each time step according to their positions and cell ids so the first particle in the first cell will be re-numbered to zero and other particles will be re-numbered respectively. This process optimizes the lookups distances and improves the coherence of access memory since the particles with close numbers tend to be close together in space. This optimization was first applied on "Particles" example of the CUDA toolkit (Green 2008) and is also used in GPUSPH model [8]. Sorting and re-ordering are not essential for fixed nodes since their positions are not changing during computational time.

When each node is assigned to a hash value, the neighbouring moving particles, which are in node's vicinity, will be considered. The position of moving particles and their hash id are already captured so searching will be applied to the neighbouring cells.

Fluid parameters on the nodes are calculated using original SPH integration formula, which is applied over the fluid parameters of nodes' neighbouring moving particles:

$$A_p = \sum_p m_p \frac{A_p}{\rho_p} W(|r_n - r_p|, h) \quad (4)$$

where notation n corresponds to the fixed nodes, notation p corresponds to the moving particle and A can be any fluid parameter such as velocity, pressure or density. The fixed nodes don't contribute in the process of finding forces

so they can be assumed as imaginary nodes, which are not participating in flow simulation, but their characteristics are computed using the characteristics of moving particles. Figure.1 shows the interaction of fixed nodes and moving particles. Black dots show the centre of moving particles and red dots show the centre of fixed nodes (In Figure.1 only one node is illustrated due to better visibility).

Second approach is to treat the fixed measurement locations as a kind of particle. In the GPUSPH model, particles can be of numerous kinds: FLUIDPART, BOUNDPART (fixed boundary particles), GATEPART (moving gate with specified velocity), PISTONPART (for moving object with specified displacement), and PADDLEPART (for flap wavemakers). For fixed measurement points, a new kind of particle can be introduced that does not contribute to the neighbor search of other particles but the neighbor search is applied for them. The fluid parameters for these points can be also calculated based on equation 4. This approach is easier and needs less changes to the existing GPUSPH model but, on the other hand, since the fixed nodes are treated as a kind of particle, larger memory allocation is needed and it's harder to optimize the computational expenses. This approach can be useful when a small number of fixed points are defined, but in our case where depth-averaged parameters are wanted, the first approach, which allows us to have a large number of fixed nodes, is applied.

The final model is capable of finding fluid parameters on Eulerian fixed points as well as Lagrangian moving particles. In post-processing, time-averaging over the wave period (to determine wave-mean values) and depth-averaging are carried out to determine the nearshore circulation.

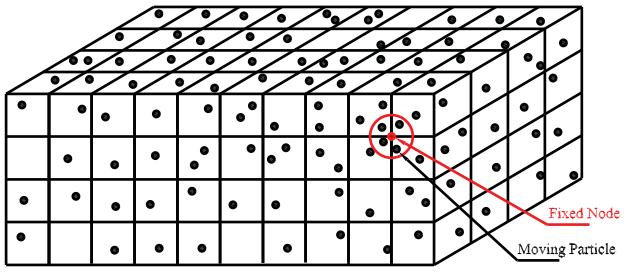

Figure 1. Schematic computational domain and the position of fixed nodes and moving particles

IV. RIP CURRENT SYSTEM

In order to model a rip current system, an idealized bathymetry consists of a single bar and a rip channel is considered. This bathymetry is based on the wave tank experiments of Drønen (2002). This experiment is chosen based on the fact that not only depth-integrated flows are investigated but also three-dimensional structure of flows in the rip current system is studied, leading to a better understanding of the physical process in different directions. Also the numerical modelling of this experiment has a reasonable computational cost.

The Drønen experiment models a half of rip current system, that is, in the longshore direction, half of a sand bar and half of a rip channel. The side walls of the wave tank correspond to lines of symmetry of a complete rip channel system. This experiment was performed in a 4 m wide and 30 m long wave tank. The bar is 4.8 m long, 3 m wide and 0.13 m high and has a slope of 1/27 in cross-shore direction. The width of the rip channel is 1 m and has the same slope of 1/27. Bar and rip channel are connected to the beach with a trough region that has 1.9 m length. The beach has a slope of 1/17. Figure 2 illustrates the plan view and side view of bed topography of the Drønen experiment.

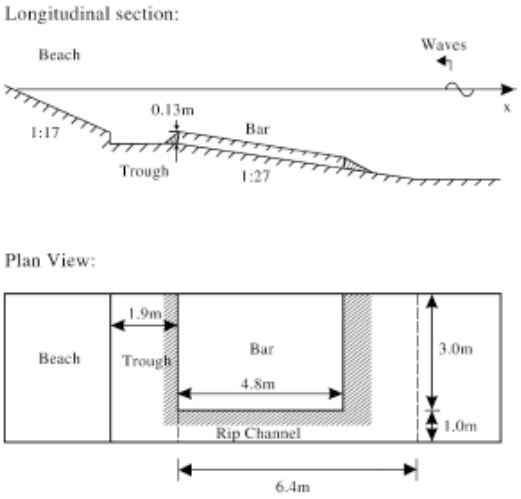

Figure 2. Rip current system bathymetry. Top: side view. Bottom: plan view [3]

In our model, the still water depth at the bar crest is 0.15 m, wave height is 0.19 m and wave period is equal to 1.5 s. Wave are generated by a wave maker which is located about 8 m far from the bar. This idealized bathymetry is modelled using extended GPUSPH model using about two and half million fluid particles and one million fixed nodes. A piston wave maker is considered as the wave generator and Wendland kernel function, with a smoothing length equal to 1.3 times particle spacing, is used as the weighting function in SPH formulation. Shepard filtering is implied every 20 time steps in order to reinitialize particles density for better results. SPS formulation is used to consider the viscous effects and Monaghan and Kajtar boundary condition [6] is implemented to provide forces in boundary particles. Variable time step, which is controlled by Courant and viscous criteria, is used. Neighbor list is updated every ten iterations. Figure 3 shows the bed topography, where the wave maker is in the right hand side and beach is located on the left hand side.

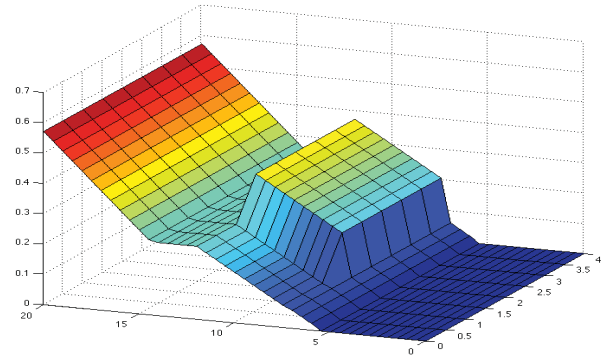

Figure 3. Bottom topography applied to the numerical code

V. NUMERICAL RESULTS AND COMPARISON WITH EXPERIMENTAL DATA

In order to find wave-induced horizontal velocity circulation at specific time steps, fluid parameters are calculated for moving particles using SPH method, then velocities at Eulerian fixed nodes are calculated using SPH interpolation and the method mentioned in the previous sections. Water surface in different locations of the rip current system and in different time steps is found. Then velocity is averaged spatially in depth from the bottom of the tank to the water surface using the velocities calculated at fixed nodes and also it is averaged over one wave period to find the mean velocity distributions. The results are examined after the wave generator was running for at least 10 waves to eliminate start-up errors. Figure 4 shows a snapshot of numerical results (visualization by Templeman Automation). This figure illustrates a side view (at top of figure) and a plan view (bottom of figure) of rip current system with the sand bar in almost middle left and a rip channel at the right. Waves are coming out of wave generator and traveling (from right hand side to the left in the top figure and from back to front in the bottom figure) until they reach the beach.

The waves break on the bar while there is almost no breaking in the rip channel. The decrease in radiation stresses (momentum flux) of the waves over the bar lead to a mean water level setup and generates a strong current flow within the rip channel, travelling seaward. Wave-current interaction in the form of refraction/diffraction, due to the propagation of wave in the inhomogeneous media (because of the presence of bar and rip channel) can also be observed. This can be seen on the front left side of the bottom figure where a pattern of diffracted waves is shown. This diffraction pattern was also observed in numerical studies of Chen et al. (1999).

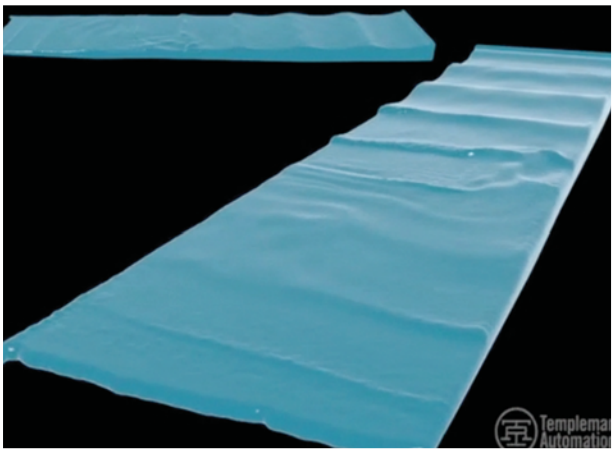

Figure 4. SPH numerical modeling of rip current. Note the wave breaking on the bar (on the left side), the wave-current interaction over the rip channel, and the wave refraction and diffraction.

A snapshot of velocity profile (plan view) at 40 s (after about 27 waves) is given in Figure 5. Waves are coming from the right hand side of the picture and red colour corresponds to higher velocity. Breaking waves can be observed on the bar. As it can be seen there is a nonuniform pattern of breaking waves on the bar that leads to differences in set-up and produces the cell circulation over the bar which will be discussed later. Waves seem to break more at the end of the bar (left hand side) so the set-up in this region becomes the main feeder of rip current in the channel.

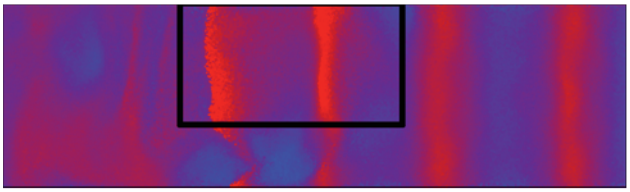

Figure 5. Plan view snapshot of flow over the bar and in rip channel at time = 40 s. Red means higher velocity, mostly associated with the breaking waves. The deformation of the wave crests by the rip current is shown.

A. Mean flow circulations

Mean horizontal velocity distribution in both numerical and experimental models is given in figure 6. In this picture, wave generator is located outside of the figure to the right hand side and waves are traveling from right to left. In the Drønen experiment (probably because of experimental restrictions), the velocity, measured at one third of the depth, is considered to be the mean velocity but in numerical simulation, the actual mean velocity is obtained by taking the average of velocity in depth.

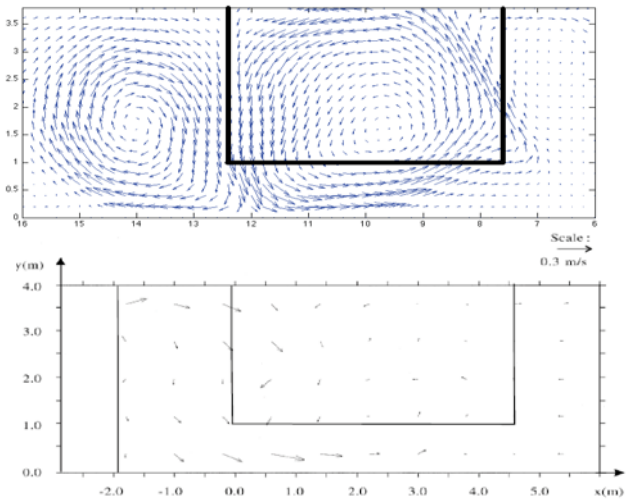

Figure 6. Mean horizontal velocity distribution. Top: Numerical results. Bottom:Expreimental result

The rip current system consists of:

- Offshore-directed rip current in the channel
- A circulation cell over the bar, which includes the rip current
- An onshore oppositely-rotating circulation cell

The circulation cell over the bar appears due to differences in set-up shoreward of the bar and in the rip channel. The second cell on the beach, which has the opposite direction to the first circulation cell, is not obviously observed in this part of Drønen experiment. That can be related to insufficient measurement locations near the beach or the fact that the mean velocities are approximated by the velocities at one third of the depth. But later during the dye injections observations of Drønen experiments, the oppositely-rotating cell on the beach was observed. This beach circulation cell was also found in Haller et al. (2002) experiments.

The rip current, at the seaward end of channel, tends to move back onto the bar and participate in the cell circulation over the bar region. The Drønen experiments were designed to study two-dimensional and three-dimensional flow patterns over the bar and in rip channel, but because of the fact that the rip current flow is bounded on one side by the sidewall, the meander-like transients of rip current (an instability examined by Haller and Dalrymple [9]), offshore of the bar, cannot be observed.

Mean surface elevation is also measured numerically and compared with the experimental data. Figure 7 illustrates the mean surface water elevation and corresponding gradients. Changes of elevations are shown using a colour domain changing from lower elevations in blue up to higher elevations in red.

Waves are coming from right hand side to the left and they are moving uniformly until they reach the bar so mean surface water elevation has low amount on the right side of the figure. When the waves travel over the bar, a nonuniform pattern of breaking happens. Waves are mostly breaking at the end of bar (left side of bar) and more close to the sidewall. So the decrease in momentum flux due to breaking leads to mean water level set-ups, which are higher at top-left side of the bar. The gradient in mean water elevations derives a current starting over the bar, flowing into the rip channel and returning back towards the sea.

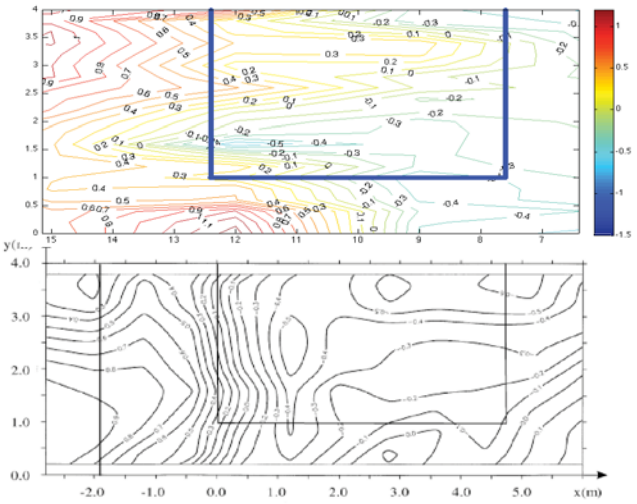

Figure 7. Mean surface elevation in cm. Top: Numerical results. Bottom:Experimental result

In order to look more accurately at the circulations and their changes during time, vorticity is calculated from GPUSPH and studied at different times. Figure 8 shows the vorticity and velocity profiles. The circulation patterns and centre of them are given in this figure more vividly. The top figure corresponds to time equal to 20 s and the bottom one corresponds to time equal to 40 s. In both of the pictures, two main circulations: one over the bar (rotating anti-clockwise) and one near-shore (rotating clock-wise) are observed but their strength and centre of rotation are changing with time. Rip current intensity is also changing with time. Two minor circulations: one on the up-right hand side of bar circulation (in the opposite direction of it) and one on the left-down side of near-shore circulation (in the opposite direction of it) can also be observed. Changes of vorticity near bottom sidewall are related to boundary effects of sidewall.

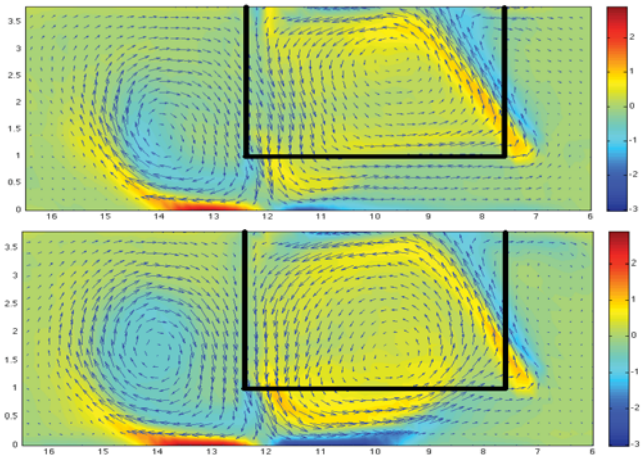

Figure 8. Mean vorticity and mean horizontal velocity distributions in Mean vortivity and mean horizonatl velocity distributions in two different times, top: T=20s, bottom: T=40s

B. *Three-dimensional structure of flow*

Depth-averaged mean velocity profiles are not always sufficient to study the flow in different parts of rip channel. Three-dimensional analysis gives a better understanding of flow development and current pattern. In order to study long-shore variation of rip current intensity, at the beginning of the rip channel (x=11.4 m), cross-shore mean velocity (averaged in time) is calculated. The result is plotted in Figure 9. The cross-shore velocity starts from the least amount (at y=0 m) and increases almost linearly towards the sidewall (at y=1 m) so the maximum rip current velocity occurs near the sidewall.

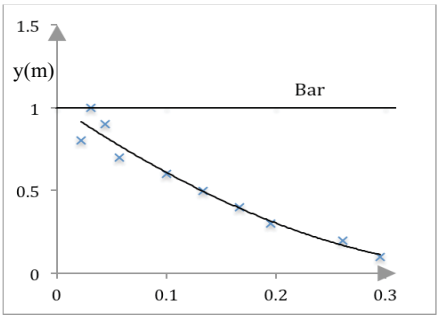

Figure 9. The cross-shore velocity as a function of long-shore position at x=1 m, at one third of the depth. x is experimental data.

The three-dimensional distribution of mean horizontal velocity profiles is given in figure 10. In this figure velocity in different points of bar, rip channel and on-shore part of the region is studied. Velocities have been averaged in one time period. The figure shows the lateral flow traveling cross-shore from bar to the rip channel. The rip current has a tendency to be stronger closer to the bed.

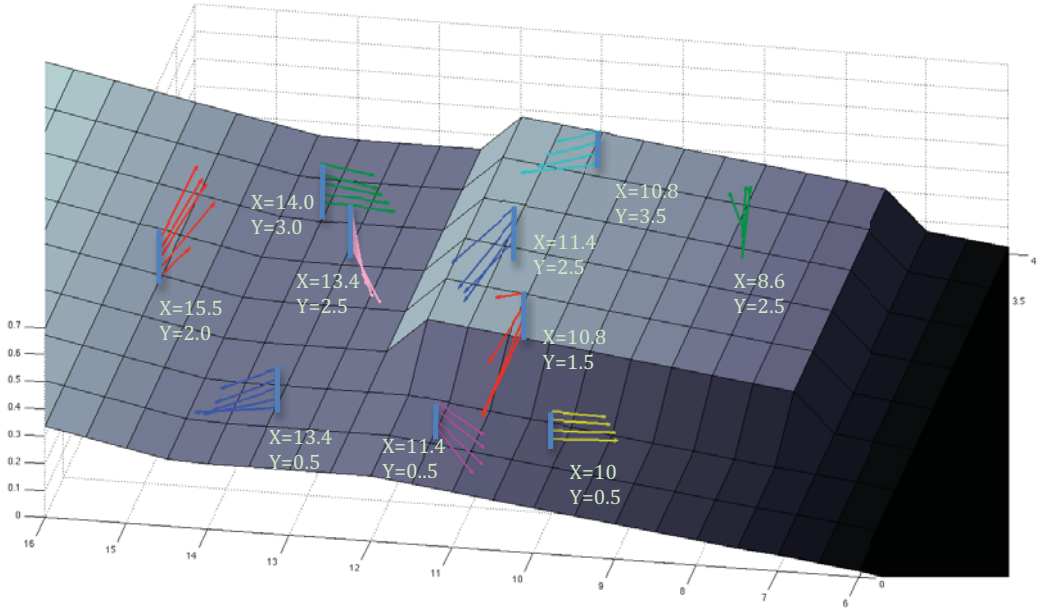

Figure 10. Three-dimensional velocity profile for Drønen et al. Test 1A.

C. *Effect of particle resolution*

Rip current modelling has been performed with different particle spacing so the suitable resolution was found. Numerical results were compared to test 3* of Drønen experiments where still water depth at the bar crest is equal to 0.1 m. Other information is similar to the previous test. Particle spacing of 0.02 m (about three million particles), 0.03 m (about seven hundred thousand particles) and 0.04 m (about three hundred thousand particles) are used. In all of the cases, circulations can be observed as is shown in figure 11 but rip current intensity is much lower in the cases with 0.03 m and 0.04 m particle spacing. In the case of 0.04 m particle spacing, almost no rip current happens in the rip channel.

Cross-shore velocities in long-shore direction of rip channel at the position of x=11.4 m and one third of the depth are studied and plotted in figure 12. The results with particle spacing equal to 0.02 m shows the best fit to experimental measurements. In cases with particle spacing equal to 0.03 m and 0.04 m, a very weak and constant rip current is observed that doesn't fit the experimental results.

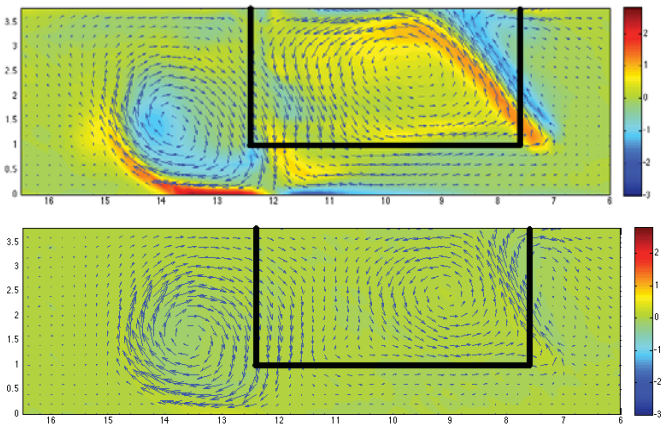

Figure 11. Effect of particle spacing on rip current modelling (Top: Particle spacing=0.02, Bottom: Particle spacing =0.04)

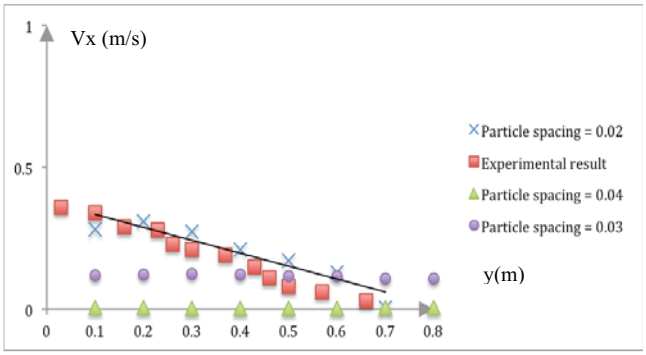

Figure 12. Effect of particle spacing on rip current modelling (Top: Particle spacing=0.02, Bottom: Particle spacing =0.04)

VI. Conclusions

The GPUSPH model of Hérault et al. [4] is extended to calculate fluid parameters at fixed Eulerian points in addition to Lagrangian moving particles. Then the model is used to model a rip current system consists of a bar and a rip channel. SPH three-dimensional modelling of the rip current system lead to a better understanding of the rip current pattern and corresponding circulation cells (one over the bar and the other one in surf zone). Wave breaking, wave/current interaction and wave diffraction are successfully modelled.

Accurate modelling of the nearshore circulation system implies that wave breaking and the wave momentum flux is modelled correctly by SPH. Mean wave-induced phenomena, such as wave set-up and wave-induced currents also are accurately modelled.

Mean horizontal velocity profiles (depth-integrated and time-integrated) and vorticity fields are investigated. Three-dimensional structure of flow in different parts of the region is observed and finally the effect of different particle spacing is considered, showing that high resolution is necessary to correctly determine flow fields and vorticity.

The model results are compared with the observations of laboratory experiments of Drønen et al. (2002). Good agreement is obtained between numerical results and experimental data in terms of mean velocity distribution mean surface elevation and three-dimensional development of currents.

VII. Acknowlegment

This work has been supported by the Office of Naval Research's Coastal Geosciences Program.

VIII. References

[1] Haller M., Dalrymple R., Svendsen I., Rip channels and nearshore circulation: experiments, Journal of Geophysical Research, vol. 107, no. C6, 2002, 3061.

[2] Chen Q., Dalrymple R., Kirby J., Kennedy A., Haller M., Boussinesq modeling of a rip current system, Journal of Geophysical Research, vol. 104, no. C9, 1999, pp. 20617-20637.

[3] Drønen N., Karunarathna H., Fredsoe J., Sumer B., Deigaard R., An experimental study of rip channel flow, 2002, Coastal Engineering, vol. 45, pp. 223-238.

[4] Hérault A., Bilotta G., Dalrymple R., SPH on GPU with CUDA, Journal of Hydraulic Research, vol. 48., 2010, pp. 74-79.

[5] Monaghan J.J., Simulating Free Surface Flows with SPH, Computational Physics, vol. 110, 1994, pp. 399-406.

[6] Monaghan J.J. and J.B. Kajtar, SPH particle boundary forces for arbitrary boundaries, Computer Physics Communications, vol. 180, 2009, pp. 1811-1820.

[7] Dalrymple R.A. and B.D. Rogers, Numerical modeling of water waves with the SPH method, Coastal Engineering, vol.53, 2006, pp. 141-147.

[8] Green S., CUDA particles, Technical report contained in the CUDA SDK, www.nvidia.com

[9] Haller, M.C. and R.A. Dalrymple, Rip current instabilities, Journal of Fluid Mechanics, vol. 433, 2001, pp. 161-192.